



## **A Study of the Flow Effect on Naphthenic Acid Corrosion of Mild Steel**

Nicolas Jauseau  
Kongsberg Oil & Gas Technologies, Inc.  
10777 Westheimer Rd. Suite 1200  
Houston, TX 77042  
USA

Srdjan Nestic  
Institute for Corrosion and Multiphase Technology  
Ohio University  
342 West State St.  
Athens, OH 45701  
USA

### **ABSTRACT**

The oil refining industry often relies on the use of easily available and cheaper crude oils rich in naphthenic acids (NAP) to improve its profit margins. However, the processing of these acidic crudes in distillation units can lead to severe corrosion issues in oil transfer lines. Moreover, it has been suggested that high flow velocities and multiphase flow conditions can enhance NAP corrosion in bends of transfer lines. To better understand the underlying phenomenon driving NAP corrosion, a flow loop was designed to mimic operating conditions encountered in the transfer lines of oil refineries. Experiments were performed to measure corrosion rates in single phase and multiphase flow conditions using metal samples with different piping geometries (straight and 90° elbow). The corrosion rates of carbon steel samples exposed to both single oil phase and gas-oil two-phase flow conditions ( $U_{SL} = 0.1-0.2$  m/s;  $U_{SG} = 0-40$  m/s) were determined using the weight loss method. This study demonstrates that the liquid refreshment rate was more important than the liquid velocity in controlling NAP corrosion in single phase flow conditions. In multiphase flow conditions, an annular-dispersed flow enhanced NAP corrosion in the pipe. In particular, the liquid film wetting the pipe proved to be more corrosive than a liquid phase transported as entrained droplets in the gas phase. The different piping geometry of the samples used to model the transfer lines did not show an effect on NAP corrosion as suggested by field observations.

**Keywords:** Multiphase flow, naphthenic acid corrosion, sulfidation corrosion, flow pattern, high flow velocity, oil refineries, transfer lines.

## INTRODUCTION

The oil refining industry often relies on the use of easily available crude oils rich in naphthenic acids (NAP) to improve its profit margins. However, these cheaper oils are corrosive and difficult to process in refineries. Various mitigation techniques<sup>1,2</sup> including neutralization, removal by pre-topping and crude oil blending, should be employed to mitigate the effects of NAP corrosion during the processing of lower quality crude oils. NAP corrosion has been observed in crude distillation units (CDUs) of oil refineries from furnace tubes to side cut piping, reboilers, atmospheric and vacuum distillation towers, and tower packing material.<sup>3,4</sup> Moreover, serious corrosion issues (*i.e.*, corrosion rates up to 12 mm/y) in bends of vacuum and atmospheric transfer lines, such as elbows, thermowells and tees, have been reported by many studies.<sup>3,5-8</sup> It is particularly interesting that transfer lines experience a combination of multiphase flow and high velocity streams.

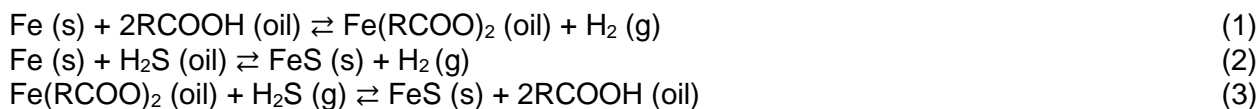
An annular-dispersed flow pattern occurring in transfer lines has been suggested to contribute to NAP corrosion.<sup>9</sup> However, there is no experimental study in multiphase flow conditions to support such hypothesis. This study seeks to closely reproduce in the lab the operating conditions encountered in transfer lines of oil refineries to study the effects of multiphase flow and piping geometry on NAP corrosion. The following sections provide insights about the NAP corrosion and the factors controlling it, introduce the new experimental flow loop designed to mimic high velocity and multiphase flow conditions, discuss the results and compare them with those obtained from different experimental approaches.

## NAPHTHENIC ACID CORROSION AND ITS CONTROLLING FACTORS

### Naphthenic Acid and Sulfidation Corrosion Mechanisms

Naphthenic acids describe a collection of organic acids containing at least one carboxylic group (COOH). The chemical structure of these acids ranges from two to six saturated rings consisting of five or six carbon atoms. This variable chemical structure dictates a wide range of physical properties, such as molecular weights (150-900 g/mol, generally 200–400 g/mol) and boiling points (200-400°C).<sup>1,4,10</sup> Consequently, the characterization of the true distribution of naphthenic acid compounds present in a particular crude oil requires the use of advanced analytical tools.<sup>11-16</sup> Pure NAP corrosion has a unique signature on bare metal surfaces, featuring “sharp-edged holes” at low flow conditions, “sharp-edged streamlined grooves” at high flow conditions,<sup>1,7</sup> and an “orange peel” like morphology in condensed vapor regions.<sup>17</sup>

Environments containing sulfur and organo-sulfur compounds lead to sulfidation corrosion that may co-exist with NAP corrosion. Although both corrosion processes are concurrent and can interact with each other, the general mechanism accepted by the corrosion community can be expressed by the following reactions:



The NAP corrosion mechanism in reaction (1) describes the attack of naphthenic acids (RCOOH) on the iron metal (Fe) producing iron naphthenates (Fe(RCOO)<sub>2</sub>), which are soluble in oil. The concurrent sulfidation corrosion mechanism in reaction (2) describes the attack of hydrogen sulfide (H<sub>2</sub>S) on iron and the formation of iron sulfide (FeS), which is insoluble in oil, and can form a scale at the steel surface. The full mechanism is completed by the regeneration of naphthenic acids and the formation of more FeS scale in reaction (3).

Many factors influence NAP corrosion, such as hydrodynamics, NAP and sulfur concentrations in oil, temperature, fluid phase and NAP boiling points, metallurgy, and time. The following section describes these factors, whereas the hydrodynamics or the flow effect on NAP corrosion is discussed separately.

### Factors Controlling the NAP Corrosiveness

The concentration of naphthenic acids present in the feedstock that is subjected to refining is an important driver of NAP corrosion. NAP concentration in oil can be expressed as the Total Acid Number (TAN), which represents the milligrams of potassium hydroxide (KOH) used to neutralize one gram of oil. Two titration standard methods, a colorimetric titration<sup>18</sup> (ASTM D 974) and a potentiometric method (ASTM D 664),<sup>19</sup> are commonly used to measure TAN, but both can lead to large discrepancies in some instances.<sup>10</sup> In spite of observed disparities, crude oils and refined fractions are considered corrosive when their TAN exceeds the limit values 0.5 and 1.5 mg KOH / g oil, respectively.

The NAP corrosivity can also be influenced by the presence of sulfur compounds in the oil. By analogy with TAN, the *total sulfur content* expressed as a total mass fraction of sulfur is used as a common factor to model the presence of sulfur species. However, not all sulfur compounds participate in the sulfidation corrosion process. H<sub>2</sub>S, either initially present in the production system or later generated by the thermal degradation of other sulfur compounds (e.g., disulfides, mercaptans), is considered to be the most reactive species. It reacts with Fe at the steel surface to produce FeS scale that can provide some level of protectiveness to hinder the attack of corrosive species.

Naphthenic acids are corrosive within the temperature range of 220-400 °C. However, their corrosiveness decreases beyond 350 °C due to thermal degradation, and is no longer observed above 400 °C in refinery environments.<sup>1,3,7,9,10,20</sup>

Several authors<sup>1,9</sup> pointed out that naphthenic acids are the most corrosive near their respective boiling points in the presence of a liquid phase. Field experience<sup>6</sup> confirmed observations of severe corrosion issues in the flashing zones. More interestingly, a previous experimental work<sup>9</sup> demonstrated that NAP corrosion was negligible in the vapor phase, while the formation of oil condensates at the surface of the metal samples located in the vapor phase led to higher corrosion rates, similar to those observed in the liquid phase. Therefore, the presence/absence of a liquid phase in contact with the wall surface could be of utmost importance in multiphase flow conditions, where both gas and oil phases can have different distribution configurations in the pipe (*i.e.*, stratified, annular, mist, slug, etc).

The duration of experimental tests involving NAP and sulfur compounds is also important to ensure that the steady state conditions can be reached and the thermal degradation of the chemical compounds due to heat exposure can be avoided.<sup>21</sup> The latter could be an issue for closed and low flow rate through systems. In general, authors<sup>21,22</sup> reported an inverse relationship between the corrosion rate and the test duration, which has been attributed to the faster kinetics of NAP corrosion relative to the slower formation of the FeS scale at the steel surface.

Oil refiners can mitigate the NAP corrosion through a better material selection. Carbon steel alloys, which are widely used in oil refineries, provide a good protection against NAP corrosion, but only at temperatures lower than 230 °C.<sup>1,4</sup> Higher chromium (5-12%<sub>wt</sub>) and molybdenum (3-4%<sub>wt</sub>) contents in steel alloys, generally provide a better protection against both NAP and sulfidation corrosion processes. Nickel based alloys with high nickel contents (65-70%<sub>wt</sub>) have also proved to be very reliable against NAP corrosion, but they are not cost-effective.<sup>1,23</sup>

### Effect of Fluid Flow on NAP Corrosion

The effect of fluid flow has been emphasized as an important controlling factor of NAP corrosion in transfer lines of oil refineries. Fluid flow and corrosion rate were previously correlated using either flow

velocity or wall shear stress, and resulted in various outcomes. Some studies<sup>20,24</sup> demonstrated a linear relationship between fluid velocity and corrosion rate, while other studies<sup>9,24,25</sup> supported the existence of a threshold value marking the onset of the flow induced NAP corrosion.

Experimentally, a higher shear stress or fluid velocity was achieved using NAP corrosive fluids in three customized apparatus: the rotating cylinder electrode (RCE), the jet impingement, and the flow loop. The RCE, on which metal samples are usually mounted, rotates in a chamber containing the corrosive medium. The external surface of metal samples can experience fluid velocities from 0.5 to 8.5 m/s and a low shear stress, while it is possible to maintain a low refreshment flow rate of the corrosive fluid in the chamber. Since high pressure was maintained in the test section to avoid flashing the oil, those experiments were always performed in single phase flow conditions.<sup>26,27</sup> The jet impingement method can generate a high velocity stream and creates much higher shear stress conditions at the target metal surface. Similar to RCE, the experimental work<sup>28-32</sup> using this method was carried out only in single liquid phase conditions, assuming that all the liquid would impinge the wall surface. This assumption may not be valid in oil refinery transfer lines. The flow loop was rarely used and only for single liquid phase conditions, because this method is technically challenging (*i.e.*, fluid management, heat losses, fluid leaks).<sup>33</sup>

Oil refinery transfer lines operate at flow velocities as high as 100-120 m/s, and with multiphase flow conditions. The existence of different flow patterns (or flow regimes) represents the paramount difference between single phase and multiphase flow systems. A flow pattern defines a given distribution of different phases (gas, liquid) flowing in the pipe and varies with the operating conditions and the pipe and fluid properties. It is characterized by different shapes of the gas-liquid interface, phase slippage, total liquid volume fraction (also called *liquid holdup*), and wetted wall fraction at the pipe wall.

## METHODS

### Experimental Equipment and Procedure - Annular Flow Rig

The main experimental apparatus, the Annular Flow Rig (AFR), presented in Figure 1, was designed to study both single oil phase and gas-oil two-phase flow effects on NAP corrosion at high temperatures similar to those encountered in transfer lines of oil refineries.<sup>34</sup> The flow loop is entirely made of stainless steel UNS S31600 for the gas lines and UNS N06625 or UNS S31600 for the oil lines. The gas phase consisted of pure carbon dioxide CO<sub>2</sub>, while the liquid phase was prepared by spiking a chemically inert mineral oil (named *white oil*) with a commercial mixture of naphthenic acids.

During an experimental test, the oil phase was pumped from the liquid storage tank, preheated to 343 °C (650 °F) and passed through a single phase test section before reaching the *gas-liquid mixing section*. Depending on high or low gas flows, the gas phase was measured by one of two rotameters mounted in parallel, preheated to 343 °C (650 °F) by four gas heaters placed in series, and bubbled through a “saturation” column containing white oil. Then, the saturated gas phase was directed to the gas-liquid mixing section to create a two-phase flow mixture. Once the multiphase flow mixture had flowed through the multiphase test section, it was cooled down by a series of three coolers before being redirected to the liquid storage tank. There, the liquid phase was recycled while the gas phase was vented out. All lines located downstream of the gas and liquid preheaters were wrapped up with heating tape and heavy insulation layers to mitigate the heat losses in the flow loop.

Two distinct horizontal test sections, a single phase flow test section and a multiphase flow test section, were set up in the flow loop to evaluate the corrosion rates (Figure 2). Tubular shaped metal samples used in the test sections were made of carbon steel UNS G10100 with a 6.35 mm (0.25 in) tubing corresponding to an inner diameter of 4.57 mm (0.18 in) and were specially machined to a length of

80.0 ± 1.1 mm (3.15 ± 0.04 in). A nomenclature was used to distinguish the different sample types: (S) for single phase flow conditions, (M) for straight and (E) for 90° elbow geometries in multiphase flow conditions. The two elbow samples (E) were made by bending two straight 80 mm tubing pieces. All samples were wrapped with heating tape and two to three insulation layers to maintain a constant temperature during the test. For each of the three sample types (S), (M) and (E), a temperature control system was used, including temperature indicators, transmitters and a temperature controller. Additionally, pressure indicators mounted downstream of the single phase test section and upstream/downstream of the multiphase flow test section helped to monitor the pressure during the test and adjust the gas flow rate if necessary. The novelty of this experimental design lies in the integration of the metal samples as part of the flow loop piping as opposed to previous studies where the samples were totally immersed in the corrosive fluid during the experiment.

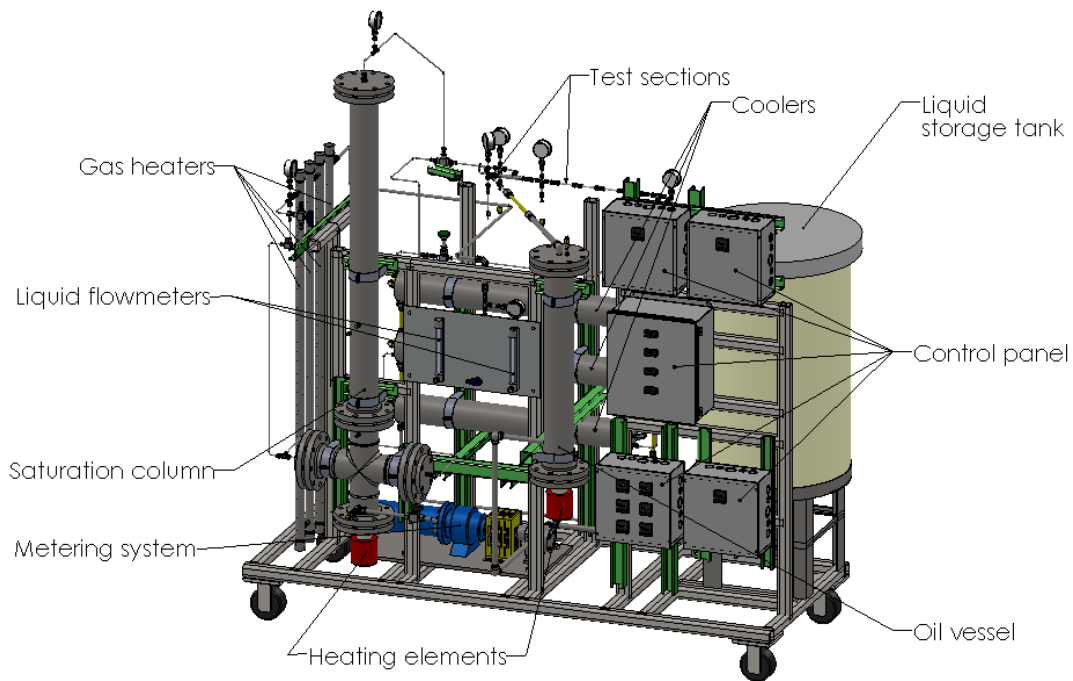


**Figure 1: Overview of the Annular Flow Rig (AFR) (Reprinted with permission from Jauseau, 2012).**

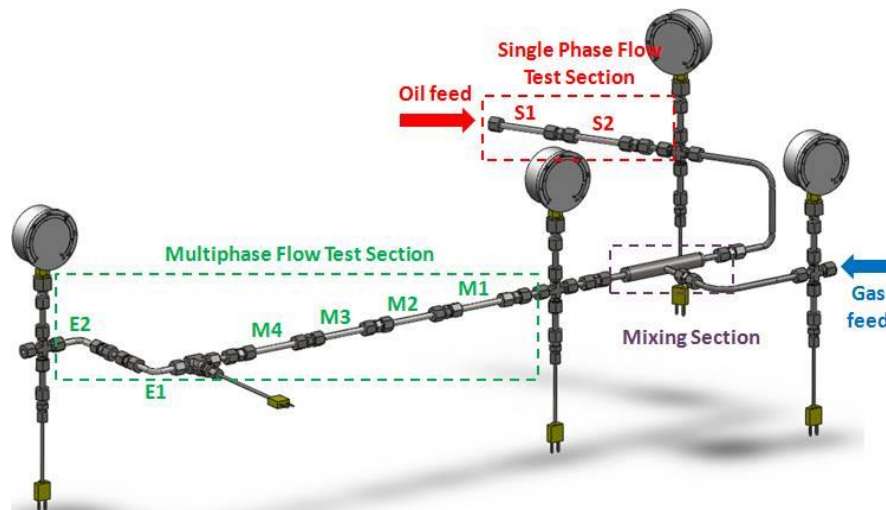


**Figure 2: Overview of the single oil phase and multiple flow test sections in the AFR flow loop (Reprinted with permission from Jauseau, 2012).**

## Experimental Equipment and Procedure - Flow Through Mini Autoclave

A separate experimental apparatus, the Flow Through Mini Autoclave (FTMA), presented in Figure 3, was used to build the FeS scale at the inner surface of the AFR samples (S, M, and E) at high temperature. The FTMA is a flow through system operating in single phase flow conditions. The liquid phase was based on a mineral oil with a natural sulfur content of 0.25 %<sub>wt</sub> (*Yellow oil*). The initial set up developed by Kanukuntla<sup>22</sup> was modified by adding an additional preheater and the combined AFR test sections<sup>34</sup> (*i.e.*, the combination of the AFR single phase and multiphase test sections). The operating temperature was maintained to 316 °C (600 °F) during the test.

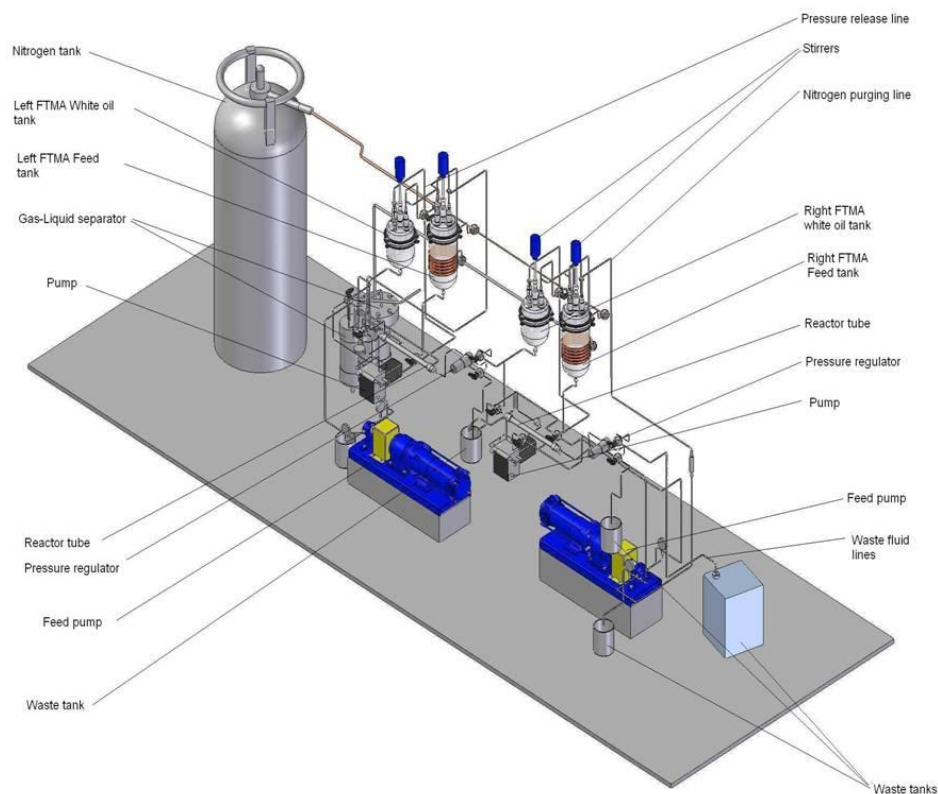


**Figure 3: Overview of the Flow Through Mini Autoclave (FTMA)<sup>38</sup>.**

### Sample Preparation

The samples used in experiments were carbon steel (CS) UNS G10100 6.35 mm (0.25 in) tubing. The CS tubing samples were polished both inside and outside under a flush of isopropanol before any testing. Outer surfaces were polished with 400 and 600 grit silicon carbide (SiC) paper. Inner surfaces were polished with a 600 grit cylinder hone mounted in a drill. After polishing, the nuts and compression fittings (front and back sleeves) were inserted in the tubing samples. Before the test, the polished samples with attached nuts and compression fittings were weighed. After the corrosion test, the metal samples were removed from the flow loop and the corrosion products formed during the test on the inner surface of the samples were mechanically and chemically removed. The mechanical removal of the scale consisted of brushing the interior with a plastic cylindrical brush, flushing with toluene and acetone, and drying with nitrogen gas. After mechanical brushing, the inner surface of the samples were flushed several times with an ASTM G1-90 solution using a plastic syringe.<sup>35</sup> Samples were weighed with an analytical balance after each step of the cleaning procedure.

## Experimental Design

### Pure NAP acid corrosion experiments

The liquid and gas flow rates were selected based on calculations for the annular flow pattern. The theoretical maximum superficial velocities of 60 m/s (single gas phase) and 2 m/s (single oil phase) in test sections could be potentially achieved. However, the experimental superficial velocity conditions were limited to 40 m/s (gas) and 0.2 m/s (oil) due to some functional limitations of the AFR parts (gas heaters, flow meters). Two different superficial liquid (oil) velocities of 0.1 m/s and 0.2 m/s were used for this experimental work. The superficial gas velocity developed in the two-multiphase flow section varied between 1.5 and 33 m/s. All experimental conditions of the pure NAP acid corrosion tests are summarized in Table 1.

### Evaluation of the FeS scale protectiveness

The FeS scale formed at the steel surface can provide a limited protection against the NAP corrosive attack. Based on experimental and field observations, a *presulfidation-challenge* procedure was used to evaluate the scale protectiveness in NAP corrosive environments. The presulfidation-challenge procedure consists of two distinct experimental phases. During the *presulfidation* phase, FeS scales formed at high temperature on the inner surfaces of metal samples exposed to real crude fractions or *model oil* compounds (with similar chemical composition as the crude fraction). During the challenge phase, the pretreated samples were exposed to a continuous NAP attack at high temperature and high fluid velocities. The procedure requires to run separate sulfidation reference tests to evaluate the metal loss corresponding to the presulfidation phase. This metal loss was subtracted from the initial weights of samples exposed to both phases to separate the effect of NAP attack on FeS scales from the corrosive effects of the presulfidation phase. Experimentally, the presulfidation phase of metal samples was performed in the FTMA. After their transfer to the AFR, the samples were challenged by a solution spiked with a commercial NAP mixture. Experimental conditions and materials used in the AFR presulfidation-challenge process are summarized in Table 1.

**Table 1**  
**Test Matrix for Pure NAP Corrosion and Presulfidation-Challenge Experiments**

Parameters	Pure NAP	Presulfidation	Challenge
Liquid phase	White oil	Yellow oil	White oil
Gas phase	CO <sub>2</sub>	-	CO <sub>2</sub>
Sample (tubing) material	Carbon steel UNS G10100	Carbon steel UNS G10100	Carbon steel UNS G10100
TAN (mg KOH / g oil)	2, 4	0.1	2, 4
Total sulfur content (% <sub>wt</sub> )	0	0.25	0
Test duration (h)	6	24	6
Temperature (°C)	343	316	343
Tubing inner diameter (mm) (in)	4.57 (0.18)	4.57 (0.18)	4.57 (0.18)
Liquid flow rate (mL/min)	80, 185	1.5	80
Superficial gas velocity (m/s) (ft/s)	0, 1.5, 10, 20, 33 (0, 4.9, 33, 66, 108)	-	0, 10, 20 (0, 33, 66)

### Corrosion Rate Calculation

Corrosion rates (CR) in this experimental work were determined with Equation (4) using the weight loss method during the tests and expressed in mm/y.

$$CR = 10 \cdot 24 \cdot 365 \cdot \frac{m_i - m_f}{\rho_{Fe} \cdot A \cdot t} \quad (4)$$

where  $m_i$  and  $m_f$  are the initial and final weights of the metal sample (g),  $\rho_{Fe}$  is the iron density ( $\text{g}/\text{cm}^3$ ) taken as  $\rho_{Fe} = 7.860 \text{ g}/\text{cm}^3$ ,  $A$  is the inner surface of the sample ( $\text{cm}^2$ ) and  $t$  is the test duration (h).

## RESULTS AND DISCUSSION

### Pure NAP acid corrosion experiments

In a pure NAP corrosion environment (TAN = 4), the corrosion rates measured in single phase flow were 6-8 times higher than those in multiphase flow conditions (Figure 4). The average corrosion rates were 12.55, 2.15 and 1.61 mm/y (494, 85 and 63 mpy) in single phase flow conditions (10 samples type S), multiphase flow conditions straight geometry (33 samples type M) and 90° elbow geometry (6 samples type E), respectively. The error bars of the corrosion rates in Figure 4 and in other figures of this section represent two standard deviations. Due to very corrosive conditions, the NAP concentration was decreased to TAN = 2. At this concentration, the corrosion rates in single phase flow conditions were reduced to 5.36 mm/y (211 mpy). Increasing the TAN concentration by a factor of 2 increased the corrosion rates by a factor of 2.3, which is in good agreement with previous experimental works.<sup>9,27</sup> In multiphase flow conditions, the NAP concentration did not show any effect on corrosion rates regardless the piping geometry of the metal sample.

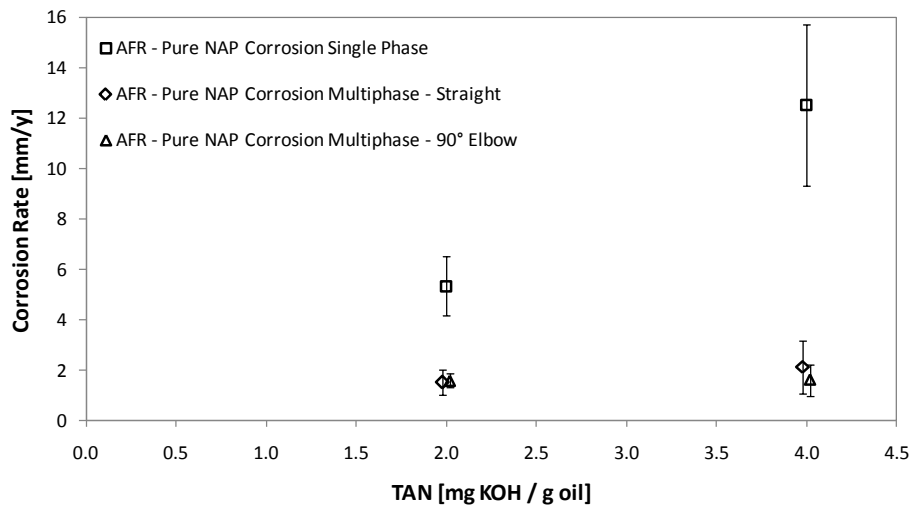


**Figure 4: Corrosion rates of non-presulfided samples with different geometries, measured for different TAN concentrations. Multiphase flow conditions are  $U_{SG} = 20 \text{ m/s}$ ,  $U_{SL} = 0.1 \text{ m/s}$ . Overlapping symbols are plotted slightly displaced for a better visualization (Reprinted with permission from Jauseau, 2012).**

Since the NAP concentration had no effect on corrosion rates of samples exposed to a multiphase flow environment, the effects of superficial gas and liquid velocities on corrosion were also investigated. The effect of superficial gas velocity on corrosion was evaluated at four different gas velocities: 1.5, 10, 20, and 33 m/s. In this test series, the liquid superficial velocity was kept constant  $U_{SL} = 0.1 \text{ m/s}$  at a NAP concentration of TAN = 2. The corrosion rates measured in the multiphase flow test section using straight and elbow geometries of the samples are plotted as a function of the superficial gas velocity in Figure 5. The highest average corrosion rate achieved was 5.4 mm/y at  $U_{SG} = 0 \text{ m/s}$  and corresponds to the corrosion rate measured in single phase conditions. As the superficial gas velocity increased from 0 to 10 m/s, the corrosion rate first decreased, then stabilized around an average value of 1.1-1.6

mm/y, while the gas velocity kept increasing up to 33 m/s. Since the liquid flow rate remained constant during the tests ( $Q_L = 80$  mL/min), the liquid holdup diminished when increasing the superficial gas velocity in the pipe.

At these operating conditions, multiphase flow modeling predicted an annular-dispersed flow regime (*i.e.*, a liquid film flowing at the pipe wall and a gas phase flowing in the pipe core with entrained liquid droplets) and a sharp increase of the liquid droplets entrainment fraction in the pipe (Figure 6). At superficial gas velocities higher than a critical threshold of  $U_{SG,crit} = 10$  m/s, the liquid phase travels in the pipe as droplets only and the flow pattern transitions into a mist flow. Below  $U_{SG,crit}$ , about 60% of the liquid flows as a liquid film at the pipe wall. The flow regime induced oil wetting of the wall promotes the NAP corrosion since a liquid (oil) phase is required for NAP corrosion to occur.

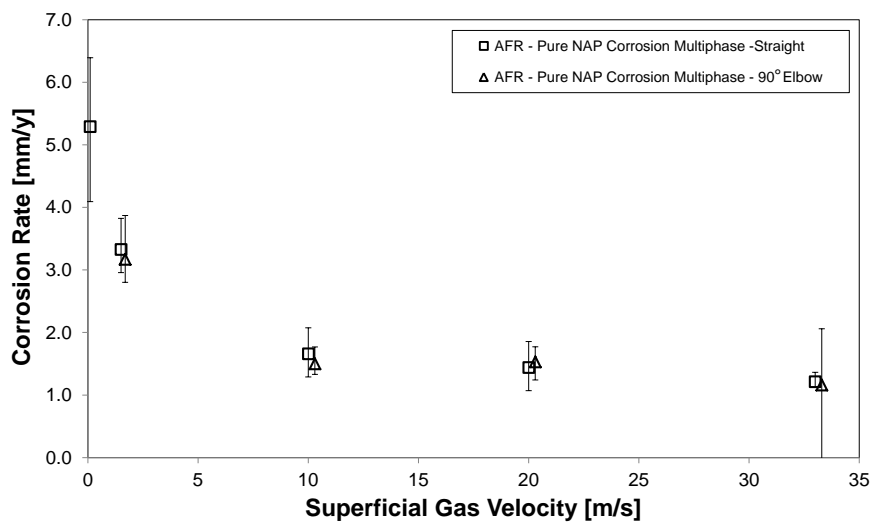


**Figure 5: Corrosion rates of non-presulfided samples of variable geometry measured at different superficial gas velocities ( $U_{SG} = 0, 1.5, 10, 20,$  and  $33$  m/s), at constant superficial liquid velocity ( $U_{SL} = 0.1$  m/s) and NAP concentration (TAN = 2). Overlapping symbols are plotted slightly displaced for a better visibility (Reprinted with permission from Jauseau, 2012).**

Early experimental work on the AFR evaluated the effect of different superficial liquid velocities on corrosion rate. At that experimental stage, no elbow samples were tested in the loop. Therefore, only corrosion rates on straight samples in multiphase flow conditions were evaluated at two different superficial liquid velocities  $U_{SL} = 0.1$  m/s and  $U_{SL} = 0.2$  m/s, corresponding to liquid refreshment rates of  $Q_L = 80$  and 185 mL/min in the test sections. For these tests, both the gas superficial velocity and the TAN concentration were kept constant at  $U_{SG} = 20$  m/s and TAN = 4, respectively. The measured corrosion rates in the multiphase flow test section are presented on the right side of Figure 7 and show that NAP corrosion was more aggressive at higher liquid superficial velocities or liquid refreshment rates (185 mL/min). From the multiphase flow perspective, a higher superficial liquid velocity increased the liquid holdup and the fraction of the liquid flowing as a liquid film at the pipe wall. The corrosion rates in multiphase flow conditions were controlled by the flow regime existing in the pipe and its characteristics, such as the wetted wall fraction of the pipe, and the entrained fraction of droplets, both informing whether the liquid phase is truly in contact with the steel surface.

In the AFR, the liquid refreshment rate (or the liquid flow rate) and the superficial liquid velocity can be considered interchangeably. However, this simple axiom no longer applies in the other apparatus (FTMA, RCEs and autoclaves). For quasi-identical experimental conditions to those encountered in the AFR (TAN = 4, T = 650 °F (343 °C)), a comparison of the corrosion rates obtained in single phase

conditions at different liquid refreshment rates is plotted on the left side (single phase) of Figure 7 along with the AFR results. In their respective test sections containing the metal samples, the autoclaves<sup>22</sup> have no refreshment rate (0 mL/min) and the FTMA with Kanukuntla's<sup>22</sup> setup has a smaller refreshment rate (1.5 mL/min). In the rotating cylinder electrode setup (HVR stands for *High Velocity Rig*), a high peripheral velocity of 8.5 m/s could be achieved at the external surface of the metal samples, but the refreshment rate of the corrosive species flushing the test section remained very low (8 mL/min).<sup>27,36</sup> The single phase flow corrosion rates measured in these four apparatus indicate a clear relationship between the corrosion rate and the refreshment rate of the corroding solution in the test section. This relationship further suggests a partial inhibition of NAP corrosion by the formation of by-products prior to be flushed away from the test section. Although the AFR samples experienced lower superficial liquid velocities (0.1 m/s in the AFR vs. 8.5 m/s in the HVR), they were exposed to a much more corrosive environment (12.55 mm/y vs. 7.94 mm/y) with a refreshment rate of the corroding fluid 10 times larger than that in the HVR. It implies that the refreshment rate is a more important controlling factor of NAP corrosion than the superficial liquid velocity (*i.e.*, the wall shear stress) in single phase flow conditions.

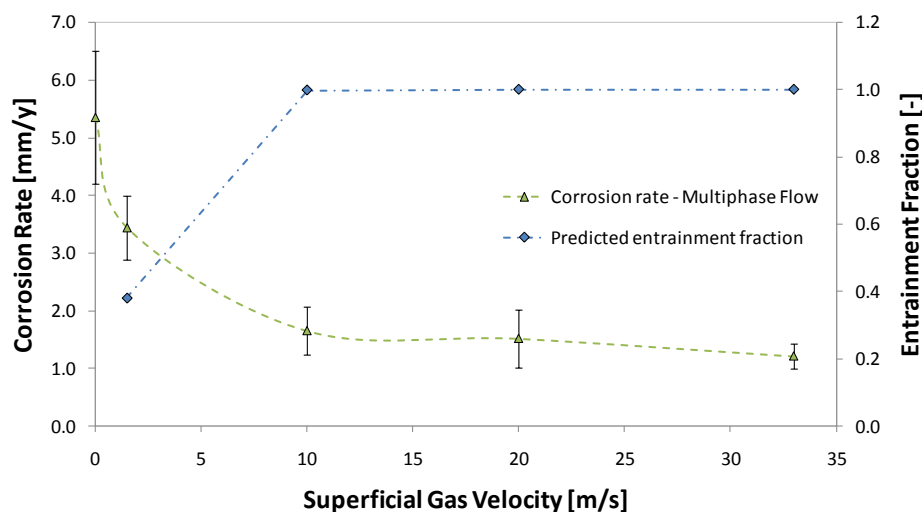


**Figure 6: Corrosion rates measured on straight samples in multiphase flow conditions and the predicted entrainment fraction of liquid droplets vs. superficial gas velocity (Reprinted with permission from Jauseau, 2012).**

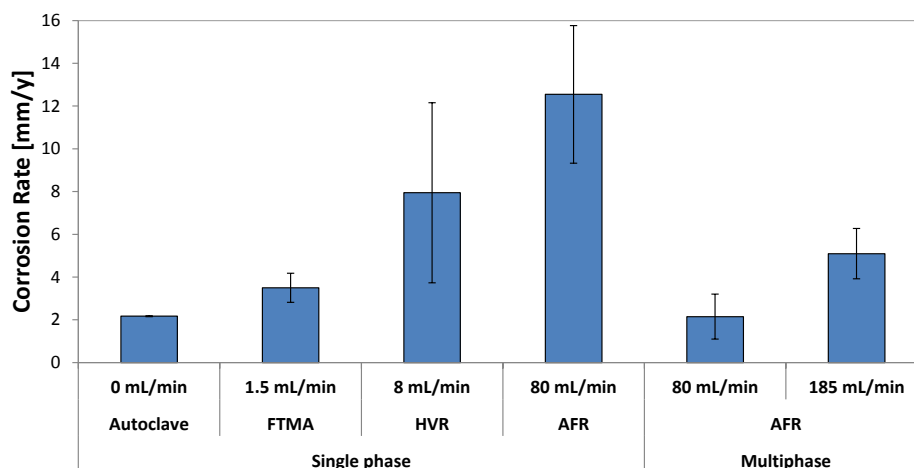


**Figure 7: Corrosion rates as a function of the liquid refreshment rate for different apparatus and fluid flow conditions at TAN 4 and 343 °C (Reprinted with permission from Jauseau, 2012).**

## Presulfidation-challenge experiments

The second part of the experimental work on the AFR investigated the protectiveness of the FeS scale against NAP corrosion under single phase and multiphase flow conditions at high temperature. Tests were performed according to the presulfidation-challenge experimental protocol with scales formed on samples using Yellow oil (Table 1). Sulfidation reference tests were performed in the FTMA and the corresponding corrosion rates are plotted on the left side of Figure 8. The duration of the presulfidation phase was 24 h, a selected time interval necessary to generate the FeS scale. Similar to pure NAP corrosion tests, the effects of TAN concentration and superficial gas velocity on corrosion rates were also studied in presulfidation-challenge tests.

The first AFR tests investigating the TAN effect on the FeS scale were done using a challenge solution of TAN 4, a gas superficial velocity of 20 m/s, and a liquid superficial velocity of 0.1 m/s. The corrosion rates of presulfided/challenged samples are presented in Figure 8. This plot reveals that the corrosion rates of presulfided samples exposed to a TAN 4 solution in single phase flow conditions were approximately 4 times higher than those of similar samples exposed to the TAN 4 challenge in the multiphase flow environment. However, the corrosion rates measured in multiphase flow conditions at TAN 4 were not influenced by the various geometry of the samples. The FeS scales formed with Yellow oil on straight and elbow samples did not show a significant protection against the TAN 4 challenge in multiphase flow conditions when compared to presulfidation corrosion rates of similar samples. This poor performance of the FeS scale in multiphase flow conditions suggested lowering the challenge TAN concentration. The corrosion rates of straight and elbow samples at TAN 2 were in the same range with those measured at TAN 4, indicating that the scale failed in protecting the metal surface even at a lower TAN challenge (Figure 8). Furthermore, at TAN 2, the piping geometry did not influence corrosion rates in the multiphase flow conditions and these corrosion rates were similar to those measured in the TAN 4 challenge tests. The effect of TAN concentration during the challenge test was only observed in single phase conditions when corrosion rates decreased significantly at TAN 2 (Figure 8).

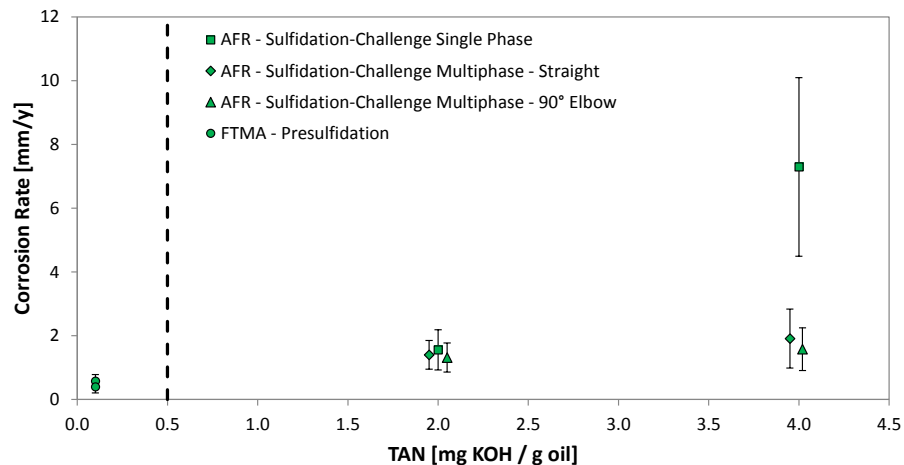


**Figure 8: Corrosion rates of presulfided samples and challenged by different TAN concentrations. Multiphase flow conditions:  $U_{SG} = 20$  m/s,  $U_{SL} = 0.1$  m/s. Average CR generated by presulfidation are plotted as references on the left side of the dashed line. Overlapping symbols are displaced for a better visualization (Reprinted with permission from Jauseau, 2012).**

The corrosion rates of presulfided and untreated samples exposed to TAN 2 and TAN 4 test solutions in single phase flow conditions are compared in Figure 9. The measured corrosion rates show that some degree of protection against NAP corrosion was offered by the FeS scale.

The corrosion rates of presulfided and untreated samples under multiphase flow conditions are compared in Figure 10. Similar to the observations made for pure NAP corrosion experiments, no effect of piping geometry was observed. Furthermore, the corrosion rates were not significantly higher as the TAN value increased, regardless the initial conditions of the samples surface (pretreated vs. non-pretreated), suggesting that the FeS scale provided no protection against NAP corrosion under multiphase flow conditions.

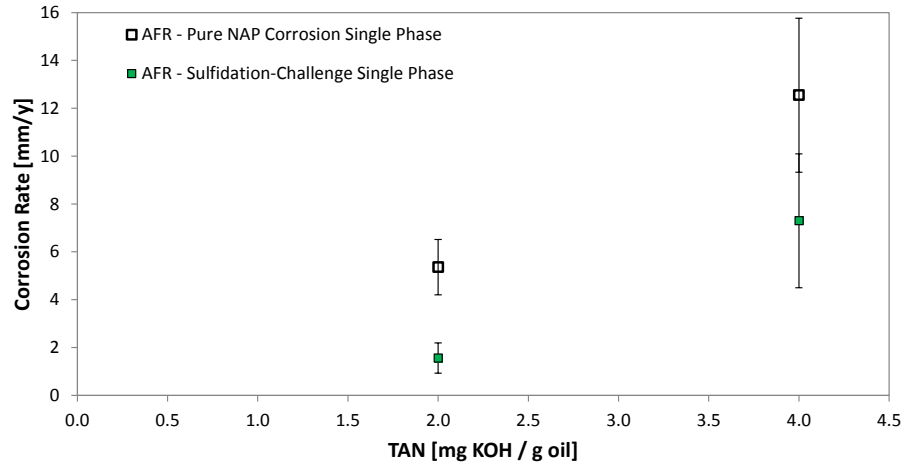


**Figure 9: Comparison of corrosion rates for non-pretreated samples and pretreated in Yellow oil. All samples were exposed to identical single phase flow conditions ( $U_{SL} = 0.1$  m/s) but using different TAN solutions (TAN 2 and 4) (Reprinted with permission from Jauseau, 2012).**

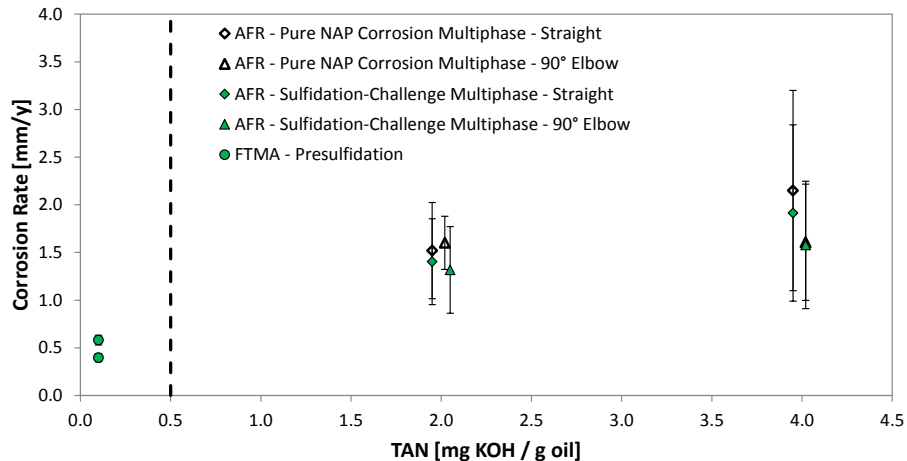


**Figure 10: Corrosion rates comparison between non-pretreated and presulfided samples. Samples with different geometries were exposed to identical multiphase flow conditions ( $U_{SG} = 20$  m/s,  $U_{SL} = 0.1$  m/s). Overlapping symbols are slightly displaced for a better visualization (Reprinted with permission from Jauseau, 2012).**

The effect of gas superficial velocity on presulfided samples exposed to NAP challenges was investigated for two superficial gas velocities ( $U_{SG} = 10$  m/s and  $U_{SG} = 20$  m/s). The superficial liquid velocity and TAN concentration were kept at  $U_{SL} = 0.1$  m/s and TAN = 2 respectively. The corrosion rates are plotted as a function of the superficial gas velocity in Figure 11. In this plot, the reference

value ( $U_{SG} = 0$  m/s) represents the average corrosion rate measured in the single phase section of the TAN 2 challenge tests on straight samples. The corrosion rates measured on straight and elbow samples did not change significantly when the superficial gas velocity increased. Results also indicate that the FeS scales formed on these samples offered the same but limited level of protection in both single phase and multiphase flow conditions. The experimental results generated in the lab for elbow samples contradicted the field observation that the most aggressive NAP attack occurred in bends.

The existence of a mist flow indicates that NAP corrosion can only occur due to droplets impingement on the pipe wall.<sup>34</sup> Furthermore, Al-Sarkhi et al.<sup>37</sup> demonstrated that the volume median diameter of droplets increases as a function of pipe diameter within a range of 0.025 - 0.095 m.<sup>37</sup> Using these observations and comparing the diameter of refinery transfer lines with the diameter of the AFR it becomes clear that the flow pattern is different under the AFR operating conditions. In the AFR, the droplets are more likely to have a smaller size distribution and, consequently, have a lower kinetic energy, insufficient to damage the FeS scale on the metal surface. In contrary, the droplets have a larger size distribution in the transfer lines of oil refineries and, therefore, a higher kinetic energy that could damage the scale and lead to higher corrosion rates.<sup>34</sup> This could explain the similar corrosion rates measured for straight and elbow samples in the AFR experiments.

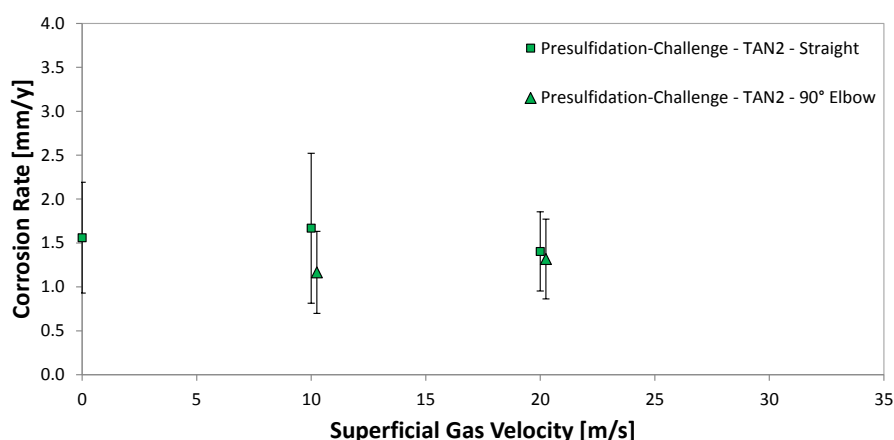


**Figure 11: Corrosion rates as a function of superficial gas velocity ( $U_{SG} = 0, 10,$  and  $20$  m/s). Samples with different geometries were presulfided prior to the challenge test with TAN = 2 experimental solution. Corrosion rate at  $U_{SG} = 0$  m/s was measured in single phase flow conditions. Overlapping symbols are slightly displaced for a better visualization (Reprinted with permission from Jauseau, 2012).**

## CONCLUSIONS

A new experimental apparatus (Annular Flow Rig) was designed and tested to perform NAP corrosion experiments at high temperature and high velocity, in single phase and multiphase flow conditions. The experiments performed in single phase flow conditions confirmed that the flow loop operates as expected. Furthermore, these tests revealed that the liquid refreshment rate of the corroding fluid is a more important factor controlling the NAP corrosion in single phase conditions than the liquid velocity or the shear stress at the pipe wall.

In multiphase flow conditions, both the measurements of corrosion rates of non-pretreated metal samples and the multiphase flow modeling demonstrated that the flow pattern developed in the test section is the main factor driving NAP corrosion. The presence of a liquid phase transported as a liquid film at the pipe wall, which is one descriptor of the annular-dispersed flow, is crucial for NAP corrosion to occur. The iron sulfide scale built on the inner surface of the metal samples using model oil did not

provide a sufficient protection against the NAP corrosive attack in multiphase flow conditions. Therefore, the experimental lab data in this study did not support an effect of piping geometry on NAP corrosion as usually observed in the field.

## ACKNOWLEDGEMENTS

The authors would like to acknowledge the sponsor of this research project and the technical support from the Institute for Corrosion and Multiphase Technology at Ohio University.

## REFERENCES

1. Derungs, W.A. "Naphthenic Acid Corrosion – An Old Enemy of the Petroleum Industry." *Corrosion*, 12 (1956): p. 617.
2. Scattergood, G.L., R.C. Strong, and W.A. Lindley. "Naphthenic Acid Corrosion, an Update of Controls Methods." CORROSION/87, paper no. 197. Houston, TX: NACE, 1987.
3. E., Blanco F., and B. Hopkinson. "Experience with Naphthenic Acid Corrosion in Refinery Distillation Process Units." CORROSION/83, paper no. 99. Houston, TX: NACE, 1983.
4. Slavcheva, E., B., Shone, and A. Turnbull. "Review of Naphthenic Acid Corrosion in Oil Refining." *British Corrosion Journal*, 34, 2 (1999): p. 125.
5. Babaian-Kibala, E., P.R. Petersen, and M.J. Humphries. "Corrosion by Naphthenic Acids in Crude Oils." 215th Nat. Meeting Am. Chem. Society. Washington, DC: American Chemical Society: Washington, DC, 1998.
6. Hopkinson, B.E., and L.E. Penuela. "Naphthenic Acid Corrosion by Venezuelan Crudes." CORROSION/97, paper no. 502. Houston, TX: NACE, 1997.
7. Jayaraman, A., H. Singh, and Y. Lefebvre. "Naphthenic Acid Corrosion in Petroleum Refineries. A Review." *Revue IFP* 41, 2 (1986): p. 265.
8. Nugent, M.J., and J.D. Dobis. "Experience with Naphthenic Acid Corrosion in Low TAN Crudes." CORROSION/98, paper no. 577. Houston, TX: NACE, 1998.
9. Gutzeit, J. "Naphthenic Acid Corrosion in Oil Refineries." *MP* 16 (1977): p. 24.
10. Piehl, R.L. "Naphthenic Acid Corrosion in Crude Distillation Units." *MP* 27 (1988): p. 37.
11. Dzidic, I., A.C. Somerville, J.C. Raia, and H.V. Hart. "Determination of Naphthenic Acids in California Crudes and Refinery Wastewaters by Fluoride Ion Chemical Ionization Mass Spectrometry." *Analytical Chemistry* 60, 13 (1988): p. 1318.
12. Hsu, C.S., G.J. Dechert, W.K. Robbins, and E.K. Fukuda. "Naphthenic Acids in Crude Oils Characterized by Mass Spectrometry." *Energy Fuels* 14, 1 (2000): p. 217.
13. Barrow, M.P., L. A. McDonnell, X. Feng, J. Walker, and P.J. Derrick. "Determination of the Nature of Naphthenic Acids Present in Crude Oils using Nanospray Fourier Transform Ion Cyclotron Resonance Mass Spectrometry: The Continued Battle Against Corrosion." *Analytical Chemistry* 75, 4 (2003): p. 860.
14. Clemente, J.S., and P.M. Fedorak. "A Review of the Occurrence, Analyses, Toxicity, and Biodegradation of Naphthenic Acids." *Chemosphere*, 60, 5 (2005): p. 585.
15. Rogers, V.V., K. Liber, and M.D. MacKinnon. "Isolation and Characterization of Naphthenic Acids from Athabasca Oil Sands Tailings Pond Water." *Chemosphere* 48, 5 (2002): p. 519.
16. Qian, K., K.E. Edwards, G.J. Dechert, S.B. Jaffe, L.A. Green, and W.N. Olmstead. "Measurement of Total Acid Number (TAN) and TAN Boiling Point Distribution in Petroleum Products by Electrospray Ionization Mass Spectrometry." *Analytical Chemistry* 80, 3 (2008): p. 849.
17. Babaian-Kibala, E., H.L. Craig, G.L. Rusk, R.C. Quinter, and M.A. Summers. "Naphthenic Acid Corrosion in Refinery Settings." *MP* 32, 4 (1993): p. 50.
18. ASTM D974 (2012). "Standard Test Method for Acid Number and Base Number by Color-Indicator Titration." West Conshohocken, PA: ASTM.

19. ASTM D664 (2011). "Standard Test Method for Acid Number of Petroleum Products by Potentiometric Titration." West Conshohocken, PA: ASTM.
20. Craig Jr., H. L. Naphthenic Acid Corrosion in the Refinery. CORROSION/95, paper no. 333. Houston, TX: NACE, 1995.
21. Turnbull, A., E. Slavcheva, and B. Shone. "Factors Controlling Naphthenic Acid Corrosion." *Corrosion* 54, 11 (1998): p. 922.
22. Kanukuntla, V., D.R. Qu, S. Nestic, and H.A. Wolf. "Experimental Study of Concurrent Naphthenic Acid and Sulfidation Corrosion." 17th Int. Corros. Congress, paper no. 2764. Houston, TX: NACE International, 2008.
23. Farraro, T., and R.M. Stellina Jr. "Materials of Construction for Refinery Applications." CORROSION/96, paper no. 614. Houston, TX: NACE, 1996.
24. Qu, D.R., Y.G. Zheng, H.M. Jing, X. Jiang, and W. Ke. "Erosion-Corrosion of Q235 and 5Cr1/2Mo Steels in Oil with Naphthenic Acid and/or Sulfur Compound at High Temperature." *Material Corrosion* 56, 8 (2005): p. 533.
25. Hau, J. L. "Predicting Sulfidic and Naphthenic Acid Corrosion." *Corrosion* 65, 12 (2009): p. 831.
26. Smart, N.R., A.P. Rance, and A.M. Pritchard. "Laboratory Investigation of Naphthenic Acid Corrosion Under Flowing Conditions." CORROSION/02, paper no. 02484. Houston, TX: NACE, 2002.
27. Bota, G.M., and S. Nestic. "Naphthenic Acid Challenges to Iron Sulfide Scale Generated "In-situ" From Model Oils on Mild Steel at High Temperature". CORROSION/13 paper no. 2512, Houston, TX: NACE, 2013.
28. Kane, R.D., and M.S. Cayard. "A Comprehensive Study on Naphthenic Acid Corrosion". CORROSION/02, paper no. 02555. Houston, TX: NACE, 2002.
29. Tebbal, S., and R.D. Kane. "Assessment of the Corrosivity of Crude Fractions from Varying Feedstock". CORROSION/97 paper no. 498, Houston, TX: NACE, 1997.
30. Wu, X.Q., H.M. Jing, Y.G. Zheng, Z.M. Yao, and W. Ke. "Corrosion and Erosion-Corrosion Behaviors of Carbon Steel in Naphthenic Acid Media." *Material Corrosion* 53, 11 (2002): p. 833.
31. Wu, X.Q., H.M. Jing, Y.G. Zheng, Z.M. Yao, and W. Ke. "Erosion-Corrosion of Various Oil-Refining Materials in Naphthenic Acid." *Wear* 256, 1-2 (2004): p. 133.
32. Wu, X.Q., H.M. Jing, Y.G. Zheng, Z.M. Yao, and W. Ke. "Study on High-Temperature Naphthenic Acid Corrosion and Erosion-Corrosion of Aluminized Carbon Steel." *Journal of Materials Science* 39, 3 (2004): p. 975.
33. Johnson, D., G. McAteer, and H. Zuk. "The Safe Processing of High Naphthenic Acid Content Crude Oils - Refinery Experience and Mitigation Studies." CORROSION/03 paper no. 03645, Houston, TX: NACE, 2003.
34. Jauseau, N. "Multiphase Flow Effects on Naphthenic Acid Corrosion of Carbon Steel." Ph.D. diss., Ohio University, 2012.
35. ASTM G 1-90 (2011). "Standard Practice for Preparing, Cleaning, and Evaluating Corrosion Test Specimens". West Conshohocken, PA: ASTM.
36. Jin, P. "Mechanism of Corrosion by Naphthenic Acids and Organo-Sulfur Compounds at High Temperatures." Ph.D. diss., Ohio University, 2013.
37. Al-Sarkhi, A., and T.J. Hanratty. "Effect of Pipe Diameter on the Drop Size in a Horizontal Annular Gas-Liquid Flow". *International Journal of Multiphase Flow* 28, 10 (2002): p. 1617.
38. Kanukuntla, V. "Formation of Sulfide Scales and Their Role in Naphthenic Acid Corrosion of Steels." Master's thesis, Ohio University, 2008.